

ARTICLE

DOI: 10.1038/s41467-018-07427-z

OPEN

Interconvertible vanadium-seamed hexameric pyrogallol[4]arene nanocapsules

Kongzhao Su¹, Mingyan Wu¹, Daqiang Yuan¹ ¹ & Maochun Hong¹

Research into stimuli-responsive controlled self-assembly and reversible transformation of molecular architectures has received much attention recently, because it is important to understand and reproduce this natural self-assembly behavior. Here, we report two coordination nanocapsules with variable cavities: a contracted octahedral V_{24} capsule and an expanded ball-shaped V_{24} capsule, both of which are constructed from the same number of subcomponents. The assemblies of these two V_{24} capsules are solvent-controlled, and capable of reversible conversion between contracted and expanded forms via control of the geometries of the metal centers by association and dissociation with axial water molecules. Following such structural interconversions, the magnetic properties are significantly changed. This work not only provides a strategy for the design and preparation of coordination nanocapsules with adaptable cavities, but also a unique example with which to understand the transformation process and their structure-property relationships.

¹State Key Laboratory of Structure Chemistry, Fujian Institute of Research on the Structure of Matter, Chinese Academy of Sciences, Fuzhou, 350002 Fujian, China. Correspondence and requests for materials should be addressed to D.Y. (email: ydq@fjirsm.ac.cn)

The design and synthesis of discrete metal-organic nanocapsules (MONCs) with specific geometries and cavities have been investigated extensively due to not only their interesting structures^{1–3}, but also their promising applications in supramolecular chemistry^{4–6} and material science^{7–9}. To date, a large number of MONCs have been synthesized from metal ions or metal clusters with different coordination environments and organic linkers with various shapes^{10–12}. Of particular recent interest is control of the self-assembly of the MONCs by external stimuli^{13,14} including light^{15,16}, electricity¹⁷, pH¹⁸, guests¹⁹, and solvents²⁰. Studies of this self-assembly may help us to understand and further mimic stimuli-responsive structural reorganization processes in biological systems. However, the structural transformations of the reported stimuli-responsive MONCs are usually accompanied by major changes in the species and number of subcomponents including metal centers and ligands. In contrast, exploration of stimuli-responsive MONCs with equal subcomponents^{21,22}, or MONC quasi-isomers^{23,24} with the same metal centers, but some different coordinated components^{15,16}, which act similarly to natural macromolecules is still in its infancy. Recognition of the reversible structural interconversion between such isomers or quasi-isomers will not only provide new approaches to broaden the preparation of MONCs with different shapes, but also an understanding of their structure–property relationships, such as host–guest recognition, drug delivery and release, and supramolecular catalysis^{16,25,26}.

C-alkylpyrogallol[4]arenes (abbreviated as PgC_n , where n is the length of the associated alkyl tail), which are vase-shaped macrocyclic host molecules composed of 1,2,3-trihydroxybenzene units, have been determined over the past decade to be versatile building blocks for the construction of supramolecular complexes²⁷. For example, PgC_n can assemble itself to form isolated MONCs^{28,29}, hydrogen-bonded capsules^{30,31}, hydrogen-bonded/metal-organic nanotubes^{32,33}, and supramolecular organic frameworks³⁴.

Since the initial discovery by Atwood et al. in 2005³⁵ of PgC_n -based MONCs constructed from six PgC_n units and 24 Cu^{2+} ions, a number of studies have demonstrated that PgC_n can self-assemble into octahedral hexameric M_{24} ($\text{M}=\text{Mg}$, Co , Ni , Cu , and Zn)^{36–40}, spherical dimeric M_8 ($\text{M}=\text{Co}$, Ni , Cu , and Zn)^{41–43}, “rugby ball” shaped hexameric Ga_{12} ⁴⁴ or mixed nanocapsules^{45–47}. Interestingly, spherical Cu_8 and Zn_8 dimers can be linked by 4,4′-bipyridine ligands into a one-dimensional coordination polymer⁴⁸ and an MOF-like structure⁴⁹, respectively. However, PgC_n -based MONCs are limited to the aforementioned metal ions, and still have the possibility of synthesizing new PgC_n -based MONCs and exerting control over their self-assembly behavior.

Vanadium is of particular interest in this context owing to its various coordination behaviors, valence states, and promising applications in areas such as magnetism^{50–52}, optics⁵³, and catalysis⁵⁴. Currently, the number of known vanadium capsules is limited^{55–58} and here we report an interesting example of solvent-responsive assembly of coordination nanocapsule quasi-isomers with distinct geometries. This includes a contracted octahedral capsule ($\text{V}_{24}\text{-oct}$) with the inner cavity of 1000 Å³, and an expanded ball-shaped capsule ($\text{V}_{24}\text{-ball}$) with inner cavity of 1400 Å³, from the same number of subcomponents including 24 vanadium centers and 6 pyrogallol[4]arene units (Fig. 1). These two V_{24} capsules represent an example of a metal displaying versatility and forming different PgC_n -based hexamer capsules.

Results

Synthesis and characterization of V_{24} octahedron and ball. C-Propylpyrogallol[4]arene (PgC_3 , Fig. 1) was synthesized as reported by Gerkenmeier et al.⁵⁹ by a condensation reaction of

pyrogallol and butanal catalyzed by concentrated hydrochloric acid. The reaction of PgC_3 with $\text{VOSO}_4 \cdot 5\text{H}_2\text{O}$ in $\text{CH}_3\text{CN}/\text{H}_2\text{O}$ solution (10:1, v/v) at 80 °C for three days yields green rhombic crystals of $\text{V}_{24}\text{-oct-}\alpha$ with the formula $[\text{V}_{24}\text{O}_{24}(\text{H}_2\text{O})_{24}(\text{C}_{40}\text{H}_{40}\text{O}_{12})_6] \cdot (\text{solvent})_x$. Single-crystal X-ray diffraction analysis shows that the $\text{V}_{24}\text{-oct-}\alpha$ crystallizes in the trigonal system with space group $R\bar{3}$ and consists of 6 PgC_3 units and 24 V ions arranged in 8 trinuclear V_3 clusters capping the face of the octahedron (Fig. 2a). The overall geometry of this capsule is similar to the previously reported octahedral hexameric M_{24} ($\text{M}=\text{Mg}$, Cu , Co , Ni , and Zn) capsules^{36–40}. Inspection of the crystal structure of $\text{V}_{24}\text{-oct-}\alpha$ reveals that each V_3 cluster is held together by three pyrogallol (Pg) units from different bowl-shape PgC_3 ligands (Fig. 2b). The angle between the two opposite upper-rim oxygen atoms and the lower-rim centroid at the base of the PgC_3 ligand is about 108.9° and the separation between two opposite faces of the octahedron, measured from the opposite centroids of the V_3 clusters is approximately 14.3 Å (Supplementary Figures 4 and 5). These three V centers adopt octahedral geometries, and each one is coordinated with four phenoxyl

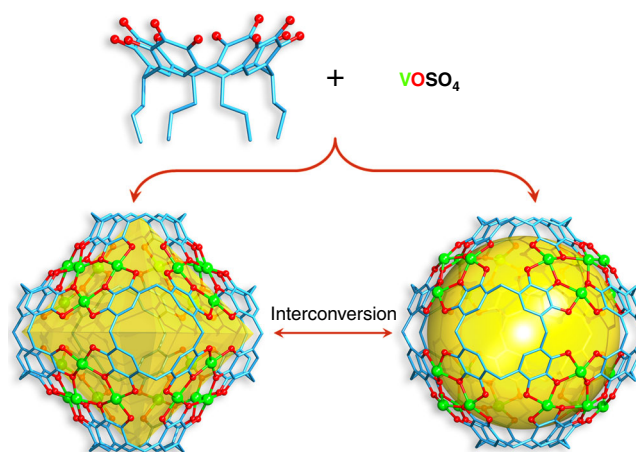


Fig. 1 Controlled self-assembly and interconversions of V_{24} capsules. Chemical structure of hexameric pyrogallol[4]arene V_{24} octahedron and V_{24} ball from 6 PgC_3 ligands and 24 vanadium ions. Vanadium is green, oxygen red and carbon blue

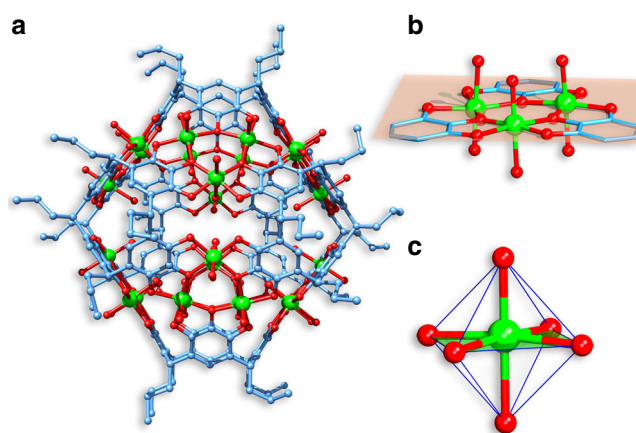


Fig. 2 Structural representations of $\text{V}_{24}\text{-oct-}\alpha$ from X-ray diffraction data. **a** Molecular structure of $\text{V}_{24}\text{-oct-}\alpha$. **b** Metal-ligand arrangement and **c** coordination geometries of V ions within the capsule

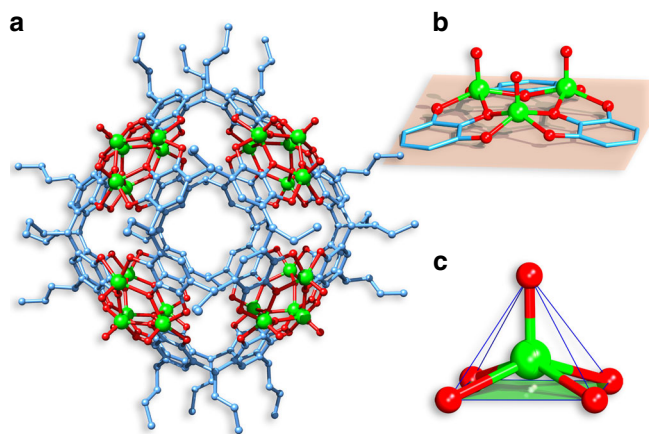


Fig. 3 Structural representations of V_{24} -ball- β from X-ray diffraction data. **a** Molecular structure of V_{24} -ball- β . **b** Metal-ligand arrangement and **c** coordination geometries of V ions within the capsule

oxygen atoms from two different PgC_3 ligands, one interior water molecule, and one exterior oxygen atom (Fig. 2c). Further analysis shows that three V centers, situated at the vertices of an approximately equilateral triangle, in which V...V distances are in the range of 3.752–3.763 Å, are linked by three phenoxyl oxygen atoms to form a planar V_3O_3 array. In this array, the V...O distances range from 1.987–2.001 Å, the O–V–O angles range from 98.18–99.09°, and the V–O–V angles range from 140.08–141.17°. The capsule contains an internal cavity with a volume of ~ 1000 Å³, calculated using VOIDOO with a probe radius of 1.2 Å. Bond valence sum (BVS) calculations and EPR analysis reveal that the vanadium centers in V_{24} -oct- α are at +4 oxidation states (Supplementary Table 2 and Supplementary Figure 1). In addition, the IR spectrum of V_{24} -oct- α shows the characteristic V=O band in the frequency range 950–990 cm⁻¹ (Supplementary Figure 2). It is interesting that the introduction of *N,N*-dimethylformamide (DMF) to the reaction of V_{24} -oct- α produces its polymorph V_{24} -oct- β which crystallizes in the triclinic space group *P*-1.

Interestingly, changing the CH_3CN/H_2O solvent in the preparation of V_{24} -oct- α to NMF/CH_3OH (1:1, v/v; *NMF*=*N*-methylformamide) affords green tetragonal prism crystals of V_{24} -ball- β : $[V_{24}O_{24}(C_{40}H_{40}O_{12})_6] \cdot (solvent)_x$, which crystallizes in the tetragonal space group *P4/mnc* and contains the same number of components as V_{24} -oct- α (Fig. 3a). This capsule can be regarded as an expanded structure of the V_{24} -oct- α for two main reasons. The angle between the two opposite upper-rim oxygen atoms and the lower-rim centroid at the base of the PgC_3 ligand has expanded to 123.1° and the separation between two opposite centroids of V_3 clusters in this ball increases to 16.7 Å, compared to V_{24} -oct- α (Supplementary Figures 4 and 5). As a result of these expansions, the inner cavity volume of the V_{24} -ball- β increases to ~ 1400 Å³, which is ~ 400 Å³ larger than the cavity in V_{24} -oct- α . Upon close examination, their structural transformations can be seen to be due to the coordination geometry differences in V centers. In this case, all the V ions are five-coordinated in square-pyramidal coordination geometries and coordinated by four phenoxyl oxygen atoms from two different PgC_3 ligands and one exterior oxygen atom (Fig. 3c). The changes of coordination geometry in the V ions have a large influence on the bond angles and the shape of the V_3O_3 array from the aforementioned V_{24} -oct- α . Specifically, the V_3O_3 array in V_{24} -ball- β is concavoconvex with V...O distances ranging from 1.953–2.037 Å, O–V–O angles ranging from 88.52–89.43° and V–O–V angles ranging from 134.38–137.12° (Fig. 3b). Except for the V...O distances, it is

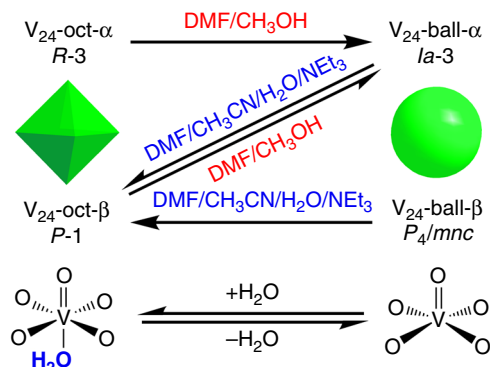


Fig. 4 The transformation mechanism of V_{24} capsules. The transformation mechanism of V_{24} octahedron and ball can be achieved by controlling the geometries of vanadium ions by association and dissociation with axial water molecules in different solvent conditions

clear that the O–V–O and V–O–V angles in this capsule are much smaller than those in V_{24} -oct- α quasi-isomer. BVS calculations and EPR analysis together with IR spectra reveal that the vanadium centers in V_{24} -ball- β are at +4 oxidation states with a VO^{2+} form (Supplementary Table 3 and Supplementary Figures 1 and 3), which are the same to those in V_{24} -oct- α . Whereas the structural differences in previously reported MONC isomers and quasi-isomers arise from the plasticity of the ligands^{15,16,21,22}, these two different types of V_{24} capsules represent an example of MONC quasi-isomers whose structural differences stem from the coordination diversity of metal centers. By replacing the NMF with DMF in the same reaction, its polymorph V_{24} -ball- α was obtained and was found to crystallize in a cubic system with the space group *Ia*-3.

Interconversions between V_{24} capsules. It has been observed that the five-coordinate square pyramidal and six-coordinated octahedral oxidovanadium complexes can interconvert by associating and disassociating an axial molecule^{60–62}. With this in mind, we searched for conditions which promote the interconversion between the contracted V_{24} octahedron and the expanded V_{24} ball. Interestingly, we found that the axial water molecules of vanadium centers in V_{24} octahedron are removed in DMF/CH_3OH (1:1, v/v) solution at 80 °C, the DMF working as a dehydrating agent;⁶³ while those vanadium centers in V_{24} ball-shaped capsule can capture the water molecules in $DMF/CH_3CN/H_2O/NEt_3$ (20:80:10:1, v/v/v/v) solution at 80 °C (Fig. 4). The dissociation and association of axial water molecules in vanadium centers lead to their coordination geometries changing from square pyramidal and octahedral forms (Fig. 2c and Fig. 3c), respectively. When the vanadium centers adopt octahedral geometry, they and the equatorial coordinated oxygen atoms from the Pg units are almost coplanar (Supplementary Figure 6a). In contrast, when adopting square-pyramidal geometries, the vanadium ions and those oxygen atoms form a curved surface (Supplementary Figure 6b). Such transformations between the plane and curved surfaces result in the changes of inner cavities from contracted octahedra to an expanded ball in V_{24} capsules. As shown in Fig. 4, V_{24} -oct- α and V_{24} -ball- β can be easily converted into V_{24} -ball- α and V_{24} -oct- β , respectively, but the reverse is not observed. However, V_{24} -oct- β and V_{24} -ball- α can interconvert by regulating the solvents, which leads to form the V_{24} capsule partners showing different shapes. To sum up, the interconversions between the contracted and expanded V_{24} capsules have been successfully achieved by a process involving

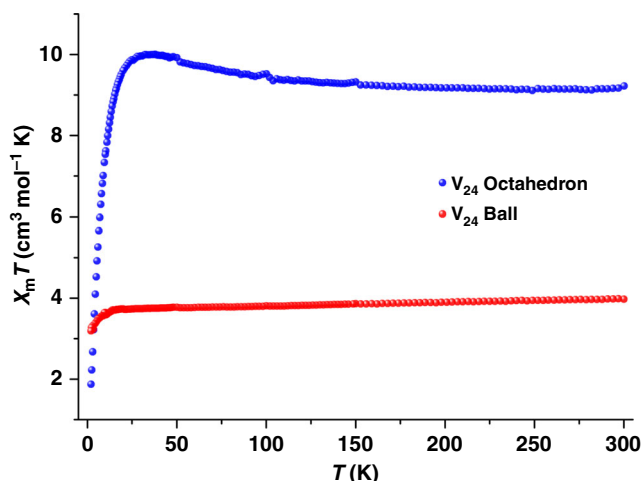


Fig. 5 Magnetic data for V_{24} capsules. Plots of $\chi_m T$ vs. T for V_{24} -oct- α and V_{24} -ball- β in a 1 kOe field

dissolution-reaction-recrystallization, which has been found to be an excellent method to explore the structural transformation of isolated coordination compounds as well as MONCs^{64–66}. However, attempts to achieve the transformations through single-crystal-to-single-crystal phase transition under the stimulation of temperature and pressure were hindered by poor crystal quality, because packing of these V_{24} capsules is via weak supramolecular interactions, and the crystals of V_{24} capsules easily lose crystallinity after partial loss of the solvent.

Magnetic properties of V_{24} capsules. Given the structural differences between these two V_{24} capsules, we compared their magnetic properties in order to yield important prototypes for exploring structure–property relationships. Here for clarity, we have provided only two phases (V_{24} -oct- α and V_{24} -ball- β) as examples, because the $\chi_m T$ vs. T data for V_{24} -oct and V_{24} -ball with two different phases show similar trends (Fig. 5 and Supplementary Figure 7). The magnetic property analyses of these two V_{24} capsules were performed on fresh samples from 2–300 K under a magnetic field of 1 kOe. For V_{24} -oct- α , the room temperature $\chi_m T$ value of $9.23 \text{ cm}^3 \cdot \text{K} \cdot \text{mol}^{-1}$ is close to the expected value of $9 \text{ cm}^3 \cdot \text{K} \cdot \text{mol}^{-1}$ for 24 spin-only V^{4+} centers^{50–52}. The value increases continuously with decreasing temperature, reaching a maximum of $10.01 \text{ cm}^3 \cdot \text{K} \cdot \text{mol}^{-1}$ at 35 K and subsequently decreases sharply to $1.88 \text{ cm}^3 \cdot \text{K} \cdot \text{mol}^{-1}$ at 2.0 K. The increase of the value of $\chi_m T$ upon reduction of the temperature at higher temperatures indicates intramolecular ferromagnetic exchange between neighboring metal ions. The 35–300 K magnetic data of this capsule was fitted to the analytical experimental equation (Eq. 1) deduced for compounds with three spin centers in an equilateral triangle⁶⁷, assuming the eight V_3 clusters are noninteracting:

$$\chi_m = \frac{N\beta^2 g^2}{4kT} \frac{1 + 5\exp(3J/2kT)}{1 + \exp(3J/2kT)} \quad (1)$$

In Eq. 1, N is Avogadro's number, β is Bohr's magneton and k is Boltzmann's constant. The best exchange interaction parameters obtained from fitting the χ_m data are $J/k = 12.38 \text{ K}$ and $g = 1.93$ (Supplementary Figure 8). The positive J value further suggests an intramolecular ferromagnetic interaction in V_{24} -oct- α at higher temperatures.

For the V_{24} -ball- β , the room temperature value of $\chi_m T$ of $3.97 \text{ cm}^3 \cdot \text{K} \cdot \text{mol}^{-1}$ is much lower than the expected value ($9 \text{ cm}^3 \cdot \text{K} \cdot \text{mol}^{-1}$) for 24 spin-only V^{4+} centers. This decreases gradually to $3.72 \text{ cm}^3 \cdot \text{K} \cdot \text{mol}^{-1}$ at $\sim 20 \text{ K}$ and then decreases rapidly reaching a value of $3.19 \text{ cm}^3 \cdot \text{K} \cdot \text{mol}^{-1}$ at 2 K. Analysis of the V_{24} -oct- α using the same equation (Eq. 1) yields $J/k = -653.8 \text{ K}$ and $g = 2.04$ (Supplementary Figure 9). Both the curve and negative J indicate dominant antiferromagnetic exchange interactions within this capsule since $\chi_m T$ at 300 K is much smaller than the expected values from 24 isolated V^{4+} spin carriers⁶⁸. Notwithstanding all V centers being at +4 oxidation states in both V_{24} capsules, the variations between the five-coordinated square-pyramidal geometries in the V_{24} -ball- β and the six-coordinated octahedral geometries in the V_{24} -oct- α are indicative of a sensitive magnetic behavior of V^{4+} centers in different ligand field environments. Neither an obvious hysteresis loop or peaks for the out-of-phase component are observed for both capsules (Supplementary Figures 10–13), and this reveals no single molecule magnetic behavior above 2 K for both capsules.

Discussion

We have developed a strategy for the efficient construction of MONC quasi-isomers by controlling the coordination environments of the metal centers. In the present case, the adoption of octahedral and square-pyramidal geometries of vanadium centers results in a contracted V_{24} octahedron and an expanded V_{24} ball, respectively. V_{24} -oct- β is the key motif in the interconversion between the contracted and expanded V_{24} capsules, which can be obtained by introducing DMF to the reaction of V_{24} -oct- α and can also be prepared from V_{24} -ball. The interconversions between V_{24} -oct- β and V_{24} -ball- α achieved by regulating solvents, leads to formation of the V_{24} capsule partners with different shapes. This work thus represents an example of MONCs whose structural differences arise from the coordination diversity of metal centers.

Methods

Materials and equipment. All reagents and solvents used in synthetic studies were obtained from commercial sources and employed without further purification. IR spectra were recorded in the range $4000\text{--}400 \text{ cm}^{-1}$ with a Magna 750 IR spectrometer using KBr pellets. Electron paramagnetic resonance (EPR) spectra were recorded on a Bruker ER-420 spectrometer with a 100 kHz magnetic field in the X band at room temperature. Magnetic susceptibilities were determined on a Quantum Design PPMS-9T and MPMS-XL systems in the range of 2–300 K. All experimental magnetic data were corrected for the diamagnetism of the sample holders and of the constituent atoms according to Pascal's constants. IR, EPR spectra and magnetic data were measured on the V_{24} -oct- α and V_{24} -ball- β samples.

Synthesis of PgC_3 ligand. A solution of pyrogallol (20 g, 160 mmol) in ethanol (100 mL) and concentrated hydrochloric acid (10 mL) was mixed dropwise with butyraldehyde (11.4 g, 160 mmol) under N_2 gas. This mixture was heated to reflux for 24 h, cooled, filtered, washed with water, a little cold ethanol and dried under vacuum. PgC_3 was collected as a colorless powder. (13.6 g, 47%). $^1\text{H NMR}$ (400 MHz, acetone- d_6): $\delta = 0.95$ (12H, t, CH_3), 1.31 (8H, m, CH_2), 2.26 (8H, q, CH_2), 4.35 (4H, t, CH), 7.14 (4H, s, ArH), 7.18 (4H, s, OH), 8.09 (8H, brs, OH) ppm.

Synthesis of V_{24} octahedron. Method 1: $\text{VOSO}_4 \cdot 5\text{H}_2\text{O}$ (0.4 mmol) and PgC_3 (0.1 mmol) were added to CH_3CN (5 mL), H_2O (0.5 mL) and NEt_3 (50 μL). The mixture was sealed in an 8 mL glass vial, which was heated at 80°C for three days, affording the green rhombic crystals of V_{24} -oct- α with a low yield (8% based on the PgC_3 ligand). Enhancement of the synthetic yield can be achieved by the slow concentration of the filtrate at room temperature for one week, and in this way, the total yield of V_{24} -oct- α was subsequently raised to 68%. Method 2: $\text{VOSO}_4 \cdot 5\text{H}_2\text{O}$ (0.4 mmol) and PgC_3 (0.1 mmol) were added to DMF (1 mL), CH_3CN (4 mL), H_2O (0.5 mL) and NEt_3 (50 μL). The mixture was sealed in an 8 mL glass vial, which was heated at 80°C for 24 h. After slow concentration of the filtrate at room temperature for one week, green block crystals of V_{24} -oct- β were collected in $\sim 72\%$ yield according to the PgC_3 ligand.

Synthesis of V_{24} ball. Method 1: $\text{VOSO}_4 \cdot 5\text{H}_2\text{O}$ (0.4 mmol) and PgC_3 (0.1 mmol) were added to DMF (2 mL) and CH_3OH (2 mL). The mixture was sealed in an 8 mL glass vial, which was heated at 80°C for 24 h. After slow concentration of the

filtrate at room temperature for five days, cubic crystals of V_{24} -ball- α were collected in ~76% yield based on the PgC_3 ligand. Method 2: $VOSO_4 \cdot 5H_2O$ (0.4 mmol) and PgC_3 (0.1 mmol) were added to NMF (2 mL) and CH_3OH (2 mL). The mixture was sealed in an 8 mL glass vial, which was heated at 80 °C for 24 h. After slow concentration of the filtrate at room temperature for five days, green tetragonal prism crystals of V_{24} -ball- β were collected in ~88% yield based on the PgC_3 ligand.

Conversion from V_{24} octahedron to V_{24} ball. In an 8 mL glass vial, synthesized crystals of V_{24} -oct- α (10 mg) or V_{24} -oct- β (10 mg) were dissolved in DMF (1 mL) and CH_3OH (1 mL), and the mixture was heated at 80 °C for 48 h. The solution was allowed to stand at room temperature for ten days to obtain ~8.5 mg green cubic crystals of V_{24} -ball- α , 81% yield.

Conversion from V_{24} ball to V_{24} octahedron. In an 8 mL glass vial, synthesized crystals of V_{24} -ball- α (15 mg) or V_{24} -ball- β (15 mg) were dissolved in DMF (0.5 mL), CH_3CN (2 mL), H_2O (0.25 mL) and NEt_3 (25 μ L), and the mixture was heated at 80 °C for 48 h. The solution was allowed to stand at room temperature for one week to obtain ~12 mg green block crystals of V_{24} -oct- β , 83% yield.

Single crystal X-ray diffractions. All X-ray single crystal data for V_{24} capsules were measured on diffractometers equipped with copper micro-focus X-ray sources ($\lambda = 1.5406 \text{ \AA}$) at 100.0(2) K. Diffraction data from V_{24} -oct- α , V_{24} -ball- β and V_{24} -ball- α were measured on a SuperNova diffractometer, and that from V_{24} -oct- β was collected on Bruker APEX-II CCD. The crystal structures were resolved by direct methods and all calculations were performed on the SHELXTL-2016 program package⁶⁹. All non-hydrogen atoms were refined anisotropically with the exception of several highly disordered propyl carbon atoms and water molecules. Hydrogen atoms of the organic ligands were added in the riding model and refined with isotropic thermal parameters. Because of the diffuse electron density and the highly disordered/amorphous solvents, molecules of crystallization could not be fully located and were therefore not included for all structures (details are also provided in Supplementary Note 1). The crystal structures were treated by the “SQUEEZE” routine⁷⁰, a part of the PLATON package of crystallographic software, dramatically improving the agreement indices. We attempted to finish the refinement, but the R_1 and wR_2 factors were still high and some A-alerts were found by the (IUCr) checkCIF routine, all of which could be ascribed to the weak crystal diffraction, which is typical in giant supramolecular assemblies. Details on crystal data collection and refinement for these capsules are summarized in Supplementary Table 1.

Data availability

The X-ray crystallographic coordinates for structures reported in this article have been deposited at the Cambridge Crystallographic Data Centre (CCDC), under deposition numbers CCDC 1535802 (V_{24} -oct- α); CCDC 1811159 (V_{24} -oct- β); CCDC 1535804 (V_{24} -ball- α); and CCDC 1535803 (V_{24} -ball- β). These data can be obtained free of charge from The Cambridge Crystallographic Data Centre (CCDC) via www.ccdc.cam.ac.uk/data_request/cif.

Received: 18 May 2018 Accepted: 22 October 2018

Published online: 22 November 2018

References

- Caulder, D. L. & Raymond, K. N. Supermolecules by design. *Acc. Chem. Res.* **32**, 975–982 (1999).
- Cook, T. R. & Stang, P. J. Recent developments in the preparation and chemistry of metallocycles and metallocages via coordination. *Chem. Rev.* **115**, 7001–7045 (2015).
- Byrne, K. et al. Ultra-large supramolecular coordination cages composed of endohedral archimedean and platonic bodies. *Nat. Commun.* **8**, 15268 (2017).
- Brown, C. J., Toste, F. D., Bergman, R. G. & Raymond, K. N. Supramolecular catalysis in metal-ligand cluster hosts. *Chem. Rev.* **115**, 3012–3035 (2015).
- Pluth, M. D. & Raymond, K. N. Reversible guest exchange mechanisms in supramolecular host-guest assemblies. *Chem. Soc. Rev.* **36**, 161–171 (2007).
- Zhang, T., Zhou, L.-P., Guo, X.-Q., Cai, L.-X. & Sun, Q.-F. Adaptive self-assembly and induced-fit transformations of anion-binding metal-organic macrocycles. *Nat. Commun.* **8**, 15898 (2017).
- Kaphan, D. M., Levin, M. D., Bergman, R. G., Raymond, K. N. & Toste, F. D. A supramolecular microenvironment strategy for transition metal catalysis. *Science* **350**, 1235–1238 (2015).
- Yeung, C.-T. et al. Chiral transcription in self-assembled tetrahedral eu4f6 chiral cages displaying sizable circularly polarized luminescence. *Nat. Commun.* **8**, 1128 (2017).
- Wu, K. et al. Homochiral d-4-symmetric metal-organic cages from stereogenic ru(ii) metalloligands for effective enantioseparation of atropisomeric molecules. *Nat. Commun.* **7**, 10487 (2016).
- Dai, F. R., Sambasivam, U., Hammerstrom, A. J. & Wang, Z. Synthetic supercontainers exhibit distinct solution versus solid state guest-binding behavior. *J. Am. Chem. Soc.* **136**, 7480–7491 (2014).
- Sun, Q. F. et al. Self-assembled m24l48 polyhedra and their sharp structural switch upon subtle ligand variation. *Chem. Commun.* **2010**, 1144–1147 (2010).
- Pasquale, S., Sattin, S., Escudero-Adán, E. C., Martínez-Belmonte, M. & de Mendoza, J. Giant regular polyhedra from calixarene carboxylates and uranyl. *Nat. Commun.* **3**, 785 (2012).
- McConnell, A. J., Wood, C. S., Neelakandan, P. P. & Nitschke, J. R. Stimuli-responsive metal-ligand assemblies. *Chem. Rev.* **115**, 7729–7793 (2015).
- Wang, W., Wang, Y.-X. & Yang, H.-B. Supramolecular transformations within discrete coordination-driven supramolecular architectures. *Chem. Soc. Rev.* **45**, 2656–2693 (2016).
- Murase, T., Sato, S. & Fujita, M. Switching the interior hydrophobicity of a self-assembled spherical complex through the photoisomerization of confined azobenzene chromophores. *Angew. Chem. Int. Ed.* **46**, 5133–5136 (2007).
- Park, J., Sun, L.-B., Chen, Y.-P., Perry, Z. & Zhou, H.-C. Azobenzene-functionalized metal-organic polyhedra for the optically responsive capture and release of guest molecules. *Angew. Chem. Int. Ed.* **53**, 5842–5846 (2014).
- Frank, M. et al. Assembly and stepwise oxidation of interpenetrated coordination cages based on phenothiazine. *Angew. Chem. Int. Ed.* **52**, 10102–10106 (2013).
- Hiraoka, S., Sakata, Y. & Shionoya, M. Ti(iv)-centered dynamic interconversion between pd(ii), ti(iv)-containing ring and cage molecules. *J. Am. Chem. Soc.* **130**, 10058–10059 (2008).
- Riddell, I. A. et al. Anion-induced reconstitution of a self-assembling system to express a chloride-binding co10l15 pentagonal prism. *Nat. Chem.* **4**, 751–756 (2012).
- Stephenson, A., Argent, S. P., Riis-Johannessen, T., Tidmarsh, I. S. & Ward, M. D. Structures and dynamic behavior of large polyhedral coordination cages: an unusual cage-to-cage interconversion. *J. Am. Chem. Soc.* **133**, 858–870 (2011).
- Rizzuto, F. J. & Nitschke, J. R. Stereochemical plasticity modulates cooperative binding in a (co12l6)-l-ii cubooctahedron. *Nat. Chem.* **9**, 903–908 (2017).
- Zhang, D. et al. Anion binding in water drives structural adaptation in an azaphosphatane-functionalized feii4l4 tetrahedron. *J. Am. Chem. Soc.* **139**, 6574–6577 (2017).
- Huang, R.-W. et al. Hypersensitive dual-function luminescence switching of a silver-chalcogenolate cluster-based metal-organic framework. *Nat. Chem.* **9**, 689–697 (2017).
- Chen, Y. et al. Isomerism in au-28(sr)(20) nanocluster and stable structures. *J. Am. Chem. Soc.* **138**, 1482–1485 (2016).
- Mirtschin, S., Slabon-Turski, A., Scopelliti, R., Velders, A. H. & Severin, K. A coordination cage with an adaptable cavity size. *J. Am. Chem. Soc.* **132**, 14004–14005 (2010).
- Noh, T. H., Heo, E., Park, K. H. & Jung, O.-S. Motion of an isolated water molecule within a flexible coordination cage: Structural properties and catalytic effects of ionic palladium(ii) complexes. *J. Am. Chem. Soc.* **133**, 1236–1239 (2011).
- Kumari, H., Deakne, C. A. & Atwood, J. L. Solution structures of nanoassemblies based on pyrogallol 4 arenes. *Acc. Chem. Res.* **47**, 3080–3088 (2014).
- Dalgarno, S. J., Power, N. P. & Atwood, J. L. Metallo-supramolecular capsules. *Coord. Chem. Rev.* **252**, 825–841 (2008).
- Jin, P., Dalgarno, S. J. & Atwood, J. L. Mixed metal-organic nanocapsules. *Coord. Chem. Rev.* **254**, 1760–1768 (2010).
- Cave, G. W. V., Antesberger, J., Barbour, L. J., McKinlay, R. M. & Atwood, J. L. Inner core structure responds to communication between nanocapsule walls. *Angew. Chem. Int. Ed.* **43**, 5263–5266 (2004).
- Dalgarno, S. J., Bassil, D. B., Tucker, S. A. & Atwood, J. L. Cocrystallization and encapsulation of a fluorophore with hexameric pyrogallol[4]arene nanocapsules: Structural and fluorescence studies. *Angew. Chem. Int. Ed.* **45**, 7019–7022 (2006).
- Kumari, H., Dennis, C. L., Mossine, A. V., Deakne, C. A. & Atwood, J. L. Magnetic differentiation of pyrogallol 4 arene tubular and capsular frameworks. *J. Am. Chem. Soc.* **135**, 7110–7113 (2013).
- Kumari, H. et al. Solution-phase and magnetic approach towards understanding iron gall ink-like nanoassemblies. *Angew. Chem. Int. Ed.* **51**, 9263–9266 (2012).
- Patil, R. S., Banerjee, D., Zhang, C., Thallapally, P. K. & Atwood, J. L. Selective co2 adsorption in a supramolecular organic framework. *Angew. Chem. Int. Ed.* **55**, 4523–4526 (2016).
- McKinlay, R. M., Cave, G. W. & Atwood, J. L. Supramolecular blueprint approach to metal-coordinated capsules. *Proc. Natl Acad. Sci. USA* **102**, 5944–5948 (2005).

36. Kumari, H. et al. Controlling the self-assembly of metal-seamed organic nanocapsules. *Angew. Chem. Int. Ed.* **51**, 1452–1454 (2012).
37. Rathnayake, A. S. et al. Investigating reaction conditions to control the self-assembly of cobalt-seamed nanocapsules. *Cryst. Growth Des.* **16**, 3562–3564 (2016).
38. Zhang, C., Patil, R. S., Liu, C., Barnes, C. L. & Atwood, J. L. Controlled 2d assembly of nickel-seamed hexameric pyrogallol[4]arene nanocapsules. *J. Am. Chem. Soc.* **139**, 2920–2923 (2017).
39. Zhang, C., Patil, R. S., Li, T., Barnes, C. L. & Atwood, J. L. Self-assembly of magnesium-seamed hexameric pyrogallol[4]arene nanocapsules. *Chem. Commun.* **53**, 4312–4314 (2017).
40. Rathnayake, A. S., Barnes, C. L. & Atwood, J. L. Zinc(ii)-directed self-assembly of metal-organic nanocapsules. *Cryst. Growth Des.* **17**, 4501–4503 (2017).
41. Power, N. P., Dalgarno, S. J. & Atwood, J. L. Guest and ligand behavior in zinc-seamed pyrogallol 4 arene molecular capsules. *Angew. Chem. Int. Ed.* **46**, 8601–8604 (2007).
42. Atwood, J. L. et al. Magnetism in metal-organic capsules. *Chem. Commun.* **46**, 3484–3486 (2010).
43. Maerz, A. K., Thomas, H. M., Power, N. P., Deakynne, C. A. & Atwood, J. L. Dimeric nanocapsule induces conformational change. *Chem. Commun.* **46**, 1235–1237 (2010).
44. McKinlay, R. M., Thallapally, P. K., Cave, G. W. V. & Atwood, J. L. Hydrogen-bonded supramolecular assemblies as robust templates in the synthesis of large metal-coordinated capsules. *Angew. Chem. Int. Ed.* **44**, 5733–5736 (2005).
45. Jin, P., Dalgarno, S. J., Barnes, C., Teat, S. J. & Atwood, J. L. Ion transport to the interior of metal-organic pyrogallol[4]arene nanocapsules. *J. Am. Chem. Soc.* **130**, 17262–17263 (2008).
46. Kumari, H. et al. Strong cation center dot center dot center dot pi interactions promote the capture of metal ions within metal-seamed nanocapsule. *J. Am. Chem. Soc.* **136**, 17002–17005 (2014).
47. Jin, P., Dalgarno, S. J., Warren, J. E., Teat, S. J. & Atwood, J. L. Enhanced control over metal composition in mixed ga/zn and ga/cu coordinated pyrogallol[4]arene nanocapsules. *Chem. Commun.* **45**, 3348–3350 (2009).
48. Fowler, D. A. et al. Coordination polymer chains of dimeric pyrogallol[4]arene capsules. *J. Am. Chem. Soc.* **133**, 11069–11071 (2011).
49. Mossine, A. V. et al. Zinc-seamed pyrogallol 4 arene dimers as structural components in a two-dimensional motif. *Chem. Sci.* **5**, 2297–2303 (2014).
50. Aronica, C. et al. A mixed-valence polyoxovanadate(iii,iv) cluster with a calixarene cap exhibiting ferromagnetic v(iii)-v(iv) interactions. *J. Am. Chem. Soc.* **130**, 2365–2371 (2008).
51. Gautier, R. et al. Spin frustration from cis-edge or -corner sharing metal-centered octahedra. *J. Am. Chem. Soc.* **135**, 19268–19274 (2013).
52. Rasmussen, M. et al. Small, beautiful and magnetically exotic: {v4w2}- and {v4w4}-type polyoxometalates. *Dalton. Trans.* **45**, 10519–10522 (2016).
53. Chen, L. et al. A basket tetradecavanadate cluster with blue luminescence. *J. Am. Chem. Soc.* **127**, 8588–8589 (2005).
54. Santoni, M.-P. et al. The use of a vanadium species as a catalyst in photoinduced water oxidation. *J. Am. Chem. Soc.* **136**, 8189–8192 (2014).
55. Zhang, Z., Wojtas, L. & Zaworotko, M. J. Organic-inorganic hybrid polyhedra that can serve as supermolecular building blocks. *Chem. Sci.* **5**, 927–931 (2014).
56. Abrahams, B. F., Fitzgerald, N. J. & Robson, R. Cages with tetrahedron-like topology formed from the combination of cyclotricatechylene ligands with metal cations. *Angew. Chem. Int. Ed.* **49**, 2896–2899 (2010).
57. Mahimaidoss, M. B. et al. Homologous size-extension of hybrid vanadate capsules—solid state structures, solution stability and surface deposition. *Chem. Commun.* **50**, 2265–2267 (2014).
58. Zhang, Y.-T. et al. Anderson-like alkoxo-polyoxovanadate clusters serving as unprecedented second building units to construct metal-organic polyhedra. *Chem. Commun.* **52**, 9632–9635 (2016).
59. Gerkenmeier, T. et al. Self-assembly of 2,8,14,20-tetraisobutyl-5,11,17,23-tetrahydroxyresorc 4 arene. *Eur. J. Org. Chem.* **1999**, 2257–2262 (1999).
60. Hanson, G. R., Sun, Y. & Orvig, C. Characterization of the potent insulin mimetic agent bis(maltolato)oxovanadium(iv) (bmov) in solution by epr spectroscopy. *Inorg. Chem.* **35**, 6507–6512 (1996).
61. Liboiron, B. D. et al. New insights into the interactions of serum proteins with bis(maltolato)oxovanadium(iv): Transport and biotransformation of insulin-enhancing vanadium pharmaceuticals. *J. Am. Chem. Soc.* **127**, 5104–5115 (2005).
62. Sanna, D., Buglyo, P., Biro, L., Micera, G. & Garribba, E. Coordinating properties of pyrone and pyridinone derivatives, tropolone and catechol toward the vo2+ ion: an experimental and computational approach. *Eur. J. Inorg. Chem.* **2012**, 1079–1092 (2012).
63. Muzart, J. N. n-dimethylformamide: much more than a solvent. *Tetrahedron* **65**, 8313–8323 (2009).
64. Li, S. et al. Atom-precise modification of silver(i) thiolate cluster by shell ligand substitution: a new approach to generation of cluster functionality and chirality. *J. Am. Chem. Soc.* **140**, 594–597 (2018).
65. Ronson, T. K., Pilgrim, B. S. & Nitschke, J. R. Pathway-dependent post-assembly modification of an anthracene-edged (m4l6)-l-ii tetrahedron. *J. Am. Chem. Soc.* **138**, 10417–10420 (2016).
66. He, Y. P. et al. Water-soluble and ultrastable ti4l6 tetrahedron with coordination assembly function. *J. Am. Chem. Soc.* **139**, 16845–16851 (2017).
67. Kahn, O. *Molecular Magnetism*. (VCH, Weinheim, Germany, 1993).
68. Rasmussen, M., Naether, C., van Leusen, J., Koegerler, P. & Bensch, W. A keggin-type structure expanded by an eight-membered ring of alternating edge-sharing vo5 and vo6 polyhedra: Solvothermal synthesis, crystal structure, and magnetic properties. *Eur. J. Inorg. Chem.* **2015**, 3285–3289 (2015).
69. Sheldrick, G. M. Crystal structure refinement with SHELXL. *Acta Crystallogr. C* **71**, 3–8 (2015).
70. Spek, A. L. Single-crystal structure validation with the program PLATON. *J. Appl. Crystallogr.* **36**, 7–13 (2003).

Acknowledgements

This work was financially supported by the Strategic Priority Research Program of the Chinese Academy of Sciences (XDB20000000), Key Research Program of Frontier Sciences, CAS (QYZDB-SSW-SLH019), National Nature Science Foundation of China (21771177, 51603206 and 21390392), and the Nature Science Foundation of Fujian Province (2016J05056). We would like to thank Dr. Scott Dalgarno and Prof. Qingfu Sun for helpful discussions.

Author contributions

D.Q.Y. and M.C.H. proposed the ideas and supervised the project. K.Z.S. performed all the experiments. D.Q.Y., K.Z.S., and M.Y.W. analyzed the data and wrote the manuscript. All authors discussed the results and commented on the manuscript.


Additional information

Supplementary Information accompanies this paper at <https://doi.org/10.1038/s41467-018-07427-z>.

Competing interests: The authors declare no competing interests.

Reprints and permission information is available online at <http://npg.nature.com/reprintsandpermissions/>

Publisher's note: Springer Nature remains neutral with regard to jurisdictional claims in published maps and institutional affiliations.

 **Open Access** This article is licensed under a Creative Commons Attribution 4.0 International License, which permits use, sharing, adaptation, distribution and reproduction in any medium or format, as long as you give appropriate credit to the original author(s) and the source, provide a link to the Creative Commons license, and indicate if changes were made. The images or other third party material in this article are included in the article's Creative Commons license, unless indicated otherwise in a credit line to the material. If material is not included in the article's Creative Commons license and your intended use is not permitted by statutory regulation or exceeds the permitted use, you will need to obtain permission directly from the copyright holder. To view a copy of this license, visit <http://creativecommons.org/licenses/by/4.0/>.

© The Author(s) 2018